

# Synthesis and structural characterization of Pd(II) and Pt(II) complexes with *P*-bonded 1'-(diphenylphosphino)ferrocenecarboxylic acid

Petr Štěpnička<sup>a,\*</sup>, Jaroslav Podlaha<sup>a</sup>, Róbert Gyepes<sup>a</sup>, Miroslav Polášek<sup>b</sup>

<sup>a</sup> Department of Inorganic Chemistry, Charles University, Hlavova 2030, Prague 12840, Czech Republic

<sup>b</sup> J. Heyrovský Institute of Physical Chemistry, Academy of Sciences of the Czech Republic, Dolejškova 3, Prague 18223, Czech Republic

Received 30 July 1997

## Abstract

The title hybrid phosphine ligand (Hdpf) coordinates to Pt(II) and Pd(II) as a monodentate phosphine. In the absence of deprotonating agents, its carboxyl group remains uncoordinated to metal, but takes part in various types of hydrogen bonding. Using  $K_2MCl_4$  as the metal ion source, *trans*-square planar complexes of the  $M(Hdpf-P)_2X_2$  type ( $M=Pd, X=Cl, Br; M=Pt, X=Cl$ ) were obtained. While  $Pd(Hdpf-P)_2Cl_2$  is formed also from  $Pd(cycloocta-1,5-diene)Cl_2$ , the analogous Pt(II)–cod complex provides *cis*-square planar  $Pt(Hdpf-P)_2Cl_2$ . The *trans*-chlorides behave inconsistently on recrystallization from carboxylic acids. While acetic acid gives single crystals of the solvates  $M(Hdpf-P)_2Cl_2 \cdot 2 AcOH$ , propionic or formic acid does not form solvates with  $Pt(Hdpf-P)_2Cl_2$  at comparable conditions. Single crystal X-ray structure determination of the last four complexes revealed remarkable differences in the conformation of the ferrocenyl moiety and in inter- and intramolecular hydrogen bonding. The two isostructural solvates have molecular arrangement with solvent molecules hydrogen-bonded to the carboxyl groups of the ligand, thus saturating their hydrogen-bond capability. As can be expected, the structure of the unsolvated *trans*- $Pt(Hdpf-P)_2Cl_2$  is that of a one-dimensional polymer linked by intermolecular hydrogen bonds. Finally, the *cis*-complex is dimeric in the crystal, being joined by pairs of the peripheral carboxyls; there is a further bonding  $\pi-\pi$  interaction between the phenyl groups of the *cis*-phosphines. © 1998 Elsevier Science S.A.

**Keywords:** Palladium; Platinum; Ferrocenyl ligands; X-ray structure

## 1. Introduction

We have recently described [1] the synthesis and properties of the novel hybrid organometallic ligand, (1'-diphenylphosphino)ferrocenecarboxylic acid [ $(\eta^5-C_5H_4PPh_2)Fe(\eta^5-C_5H_4CO_2H)$ , Hdpf]. It is closely related to the series of carboxyl-substituted phosphines [2]  $Ph_{3-n}P(CH_2CO_2H)_n$  ( $n = 1-3$ ) and  $[Ph_{2-m}(HO_2CCH_2)_mCH_2-]_2$  ( $m = 1,2$ ) which, as ligands in metal complexes, induce features such as water-solubility, pH-dependent chelating vs. bridging vs. monodentate coordination, and supramolecular solid-state structures via hydrogen bonding. On introducing the ferrocenyl group into the ligand backbone, redox chemistry could be expected, which may be of interest in catalytic and other properties of metal complexes of the

ligand. This paper deals with its behaviour as a monodentate *P*-ligand towards Pd(II) and Pt(II).

## 2. Experimental

All solvents were purified by standard procedures. The following starting compounds were prepared as reported: Hdpf [1],  $[PdBr_2(cod)]$ ,  $[PdCl_2(cod)]$  and  $[PtCl_2(cod)]$  (cod is  $\eta^4$ -cycloocta-1,5-diene) [3]. The  $^1H$  (200.06 MHz),  $^{31}P\{^1H\}$  (80.98 MHz) and  $^1H, ^1H-COSY$  NMR spectra were recorded on a Varian UNITY200 instrument and the  $^{13}C$  APT (125.70 MHz) and  $^{13}C$  HMQC (observed  $^1H$  at 499.84 MHz) spectra on a Varian UNITY500 spectrometer in dimethyl sulphoxide- $d_6$  (DMSO- $d_6$ ) solutions at ambient temperature (at 30°C for HMQC). The  $^1H$  and  $^{13}C$  chemical shifts are referred to internal  $Me_4Si$  and the  $^{31}P$  shifts to external 85% aqueous  $H_3PO_4$  (Table 1). Infrared spectra were measured in the range of 400–4000  $cm^{-1}$  on an FT-IR MATTSON Genesis instrument as Nujol mulls.

\* Corresponding author. E-mail: stepnic@mail.natur.cuni.cz.

Table 1

Elemental analyses,  $^1\text{H}$  and  $^{31}\text{P}$  NMR data for  $[\text{M}(\text{Hdpf-}P)_2\text{X}_2]$  complexes ( $\text{M} = \text{Pd}(\text{II}), \text{Pt}(\text{II}); \text{X} = \text{Cl}, \text{Br}$ )

Complex	Analysis (%) <sup>a</sup>			$^{31}\text{P}^b$		$^1\text{H}^{c,d}$			
	C	H	Cl	$\delta_p$	$J(^{195}\text{Pt}, ^{31}\text{P})$ Hz	$\delta_{\text{H}}(\text{Cp-P})$	$\delta_{\text{H}}(\text{Cp-C})$	$\delta_{\text{H}}(\text{Ph-rings})$	$\delta_{\text{H}}(\text{COOH})$
<i>Trans-1</i>	54.9(54.9)	3.9(3.8)	6.8(7.1)	16.76s	–	4.52(brs, 2H), 4.54(brs, 2H)	4.76(brt, 2H), 4.89(brt, 2H)	7.44–7.67(m, 10H)	12.45(brs, 1H)
<i>Trans-2</i>	49.7(50.5)	3.2(3.5)	–	15.58s	–	4.56(brs, 4H)	4.63(brt, 2H), 4.85(brt, 2H)	7.47–7.66(m, 10H)	12.45(brs, 1H)
<i>Trans-3</i>	49.8(50.5)	3.5(3.5)	6.7(6.5)	12.49s	2620	4.54(brs, 4H)	4.75(brs, 2H), 4.90(br, 2H)	7.45–7.67(m, 10H)	12.45(brs, 1H)
<i>Cis-3</i> <sup>e</sup>	50.1(50.5)	3.3(3.5)	6.5(6.5)	9.26s	3770	4.01(brs, 2H), 4.23(brs, 2H)	3.75(t, 2H), 4.31 (t, 2H)	7.35–4.58(m, 6H), 7.68–7.84(m, 4H)	12.38(brs, 1H)

<sup>a</sup> Found (required for  $[\text{MX}_2(\text{C}_{23}\text{H}_{19}\text{PO}_2\text{Fe})_2]$ ).<sup>b</sup> 80.98 MHz, in  $\text{DMSO-}d_6$ , external reference 85% aqueous  $\text{H}_3\text{PO}_4$ . In the case of  $\text{Pt}(\text{II})$ -compounds,  $^{195}\text{Pt}$  satellites with 33% of the overall intensity.<sup>c</sup> 200.06 MHz, in  $\text{DMSO-}d_6$ , internal reference  $\text{Me}_4\text{Si}$ .<sup>d</sup> s: singlet, d: doublet, t: apparent triplet of the AA'BB' spin system, m: multiplet, br: broad.<sup>e</sup> Sample dried before analysis (120°C/5 h).

Fast atom bombardment (FAB) mass spectra were recorded on a Finnigan MAT 95 instrument in the positive ion mode. The ions produced by bombardment of the sample in a 3-nitrobenzylalcohol matrix by fast Xe-atoms (4 keV, 1 mA) are listed as the  $m/z$  values of monoisotopic species (calculated using the most abundant isotopes); the strongest peak in the isotopic mass distribution is in parentheses (Table 2). The elemental composition of the ions was confirmed by comparison of experimental spectra with the theoretical distribution. Considering the low intensity of the fragments (typically less than 1% of the matrix peaks) together with the complicated isotopic distribution, the intensity of metal-containing fragments is given in Table 2 in relative terms only: b-base, i.e. the most intense,

s-strong, m-medium, w-weak; the ion  $m/z$  414 usually exceeded the intensity of all organometallic fragments.

### 3. Syntheses

#### 3.1. *Trans-[Pd(Hdpf-P)<sub>2</sub>Cl<sub>2</sub>], trans-I*

An aqueous solution of  $\text{K}_2\text{PdCl}_4$  (65.5 mg, 201  $\mu\text{mol}$ , 1.2  $\text{cm}^3$ ) was added to a hot solution of Hdpf (166.0 mg, 401  $\mu\text{mol}$ ) in EtOH (5  $\text{cm}^3$ ). The resulting red solution was heated to boiling and allowed to stand at room temperature overnight. The solid product was filtered off, washed with hot EtOH (3  $\times$  2  $\text{cm}^3$ ),  $\text{Et}_2\text{O}$  (5  $\times$  2  $\text{cm}^3$ ) and petroleum ether (5  $\times$  2  $\text{cm}^3$ ). After drying on air, 181.8 mg (91%) of an orange microcrys-

Table 2

FAB-MS data<sup>a</sup> for  $[\text{M}(\text{Hdpf-}P)_2\text{X}_2]$  complexes ( $\text{M} = \text{Pd}(\text{II}), \text{Pt}(\text{II}); \text{X} = \text{Cl}, \text{Br}$ )

Ion	Elemental composition	<i>Trans-1</i>	<i>Trans-2</i>	<i>Trans-3</i>	<i>Cis-3</i>
$M^+$ ; $[\text{M}(\text{Hdpf})_2\text{X}_2]^+$	$\text{C}_{46}\text{H}_{38}\text{Fe}_2\text{O}_4\text{P}_2\text{MX}_2$	1004(1006)m	1092(1094)m	1093(1094)m	1094w <sup>d</sup>
$[\text{M}(\text{Hdpf})_2\text{X}]^+$	$\text{C}_{46}\text{H}_{38}\text{Fe}_2\text{O}_4\text{P}_2\text{MX}$	969(969)m	1013(1015)s	–	1058(1059)w
$[\text{M}(\text{Hdpf})(\text{dpf})]^+$ <sup>b</sup>	$\text{C}_{46}\text{H}_{37}\text{Fe}_2\text{O}_4\text{P}_2\text{M}$	933(933)m	933(933)m	1022w <sup>d</sup>	1022(1022)w
$[(\text{CpP}^* \text{Fe})(\text{Hdpf})\text{MX}_2]^+$	$\text{C}_{40}\text{H}_{33}\text{Fe}_2\text{O}_2\text{P}_2\text{MX}_2$	895(897)m	983(985)s	984(985)m	984(985)m
$[(\text{CpP}^* \text{Fe})(\text{dpf})\text{MX}]^+$	$\text{C}_{40}\text{H}_{32}\text{Fe}_2\text{O}_2\text{P}_2\text{MX}$	859(859)b	903(905)s	948(949)s	948(949)m
$[(\text{CpP}^* \text{Fe})(\text{dpf})\text{M}]^+$	$\text{C}_{40}\text{H}_{32}\text{Fe}_2\text{O}_2\text{P}_2\text{M}$	824(824)m	–	913w <sup>d</sup>	913(913)m
$[(\text{CpP}^*)(\text{dpf})\text{M}]^+$	$\text{C}_{40}\text{H}_{32}\text{FeO}_2\text{P}_2\text{M}$	769m <sup>c</sup>	–	–	857(857)w
$[(\text{CpP}^* \text{Fe})(\text{CpP}^* \text{FeCp})\text{MX-1}]^+$	$\text{C}_{39}\text{H}_{32}\text{Fe}_2\text{P}_2\text{MX}$	–	–	904(905)w	904(905)w
$[(\text{CpP}^* \text{Fe})(\text{CpP}^* \text{FeCp})\text{M-1}]^+$	$\text{C}_{39}\text{H}_{32}\text{Fe}_2\text{P}_2\text{M}$	–	–	–	869(869)w
$[(\text{CpP}^*)(\text{CpP}^* \text{FeCp})\text{M}]^+$	$\text{C}_{39}\text{H}_{33}\text{FeP}_2\text{M}$	725(725)s	725(725)s	814(814)b	814(814)b
$[(\text{CpP}^*)(\text{CpP}^* \text{Fe})\text{M}]^+$	$\text{C}_{34}\text{H}_{28}\text{FeP}_2\text{M}$	660(660)m	660(660)m	–	–
$[(\text{Hdpf})\text{MX}]^+$	$\text{C}_{23}\text{H}_{19}\text{FeO}_2\text{PMX}$	555(555)s	599(601)b	–	–
$[(\text{Hdpf})\text{M}]^+$	$\text{C}_{23}\text{H}_{19}\text{FeO}_2\text{PM}$	520(520)s	520(520)s	–	–
$\text{Hdpf}^+$	$\text{C}_{23}\text{H}_{19}\text{FeO}_2\text{P}$	414(414)	414(414)	414(414)	414(414)

<sup>a</sup> For experimental details see Section 2; P\* denotes diphenylphosphino group ( $\text{PPh}_2$ ).<sup>b</sup> Mixture of ions ( $Q, Q+1$ ); the most abundant component given in the table.<sup>c</sup>  $m/z$  769 because of presence of ion mixture ( $Q, Q+1$ ).<sup>d</sup> Very weak.

talline solid was obtained. IR,  $\tilde{\nu}/\text{cm}^{-1}$ : 1671 s, 1295 s, 1195 s, 1096 m, 1032 m, 744 s, 709 s, 509 s (composite band). For  $^1\text{H}$ - and  $^{31}\text{P}$ -NMR data, see Table 1.

The same product was obtained using  $[\text{PdCl}_2(\text{cod})]$ : a hot dichloromethane solution (5  $\text{cm}^3$ ) of Hdpf (165.2 mg, 399  $\mu\text{mol}$ ) was added to a boiling dichloromethane solution (10  $\text{cm}^3$ ) of  $[\text{PdCl}_2(\text{cod})]$  (57.3 mg, 201  $\mu\text{mol}$ ). The resulting red solution yielded, on standing overnight at room temperature, a solid that was isolated as given above to give 186.5 mg (92%) of orange microcrystalline product. The  $^1\text{H}$ ,  $^{31}\text{P}$  NMR and IR spectra were identical with those of *trans*-**1** prepared from  $\text{K}_2\text{PdCl}_4$ .

The reaction of stoichiometric amounts of  $[\text{Pd}(\text{PhCN})_2\text{Cl}_2]$  and Hdpf in hot toluene also yielded *trans*-**1**. The product, however, was contaminated with non-coordinated Hdpf as indicated by elemental analysis and  $^{31}\text{P}$  NMR.

### 3.2. *Trans*- $[\text{Pd}(\text{Hdpf-P})_2\text{Br}_2]$ , *trans*-2

A solution of  $[\text{PdBr}_2(\text{cod})]$  (76.3 mg, 204  $\mu\text{mol}$ ) in hot dichloromethane (17  $\text{cm}^3$ ) was added to a solution of Hdpf (166.9 mg, 403  $\mu\text{mol}$ ) in hot dichloromethane (3  $\text{cm}^3$ ). The mixture turned dark red and deposition of a red-brown solid started, which was allowed to stand for 24 h at room temperature; the solid residue was filtered off, washed with  $\text{CHCl}_3$  (2  $\times$  1  $\text{cm}^3$ ),  $\text{Et}_2\text{O}$  (5  $\times$  1  $\text{cm}^3$ ) and dried on air. Yield: 208.7 mg (95%) of a red-brown solid. IR,  $\tilde{\nu}/\text{cm}^{-1}$ : 1679 s, 1295 s, 1162 m, 746 m, 691 m, 507 s (composite).

### 3.3. *Trans*- $[\text{Pt}(\text{Hdpf-P})_2\text{Cl}_2]$ , *trans*-3

An aqueous solution of  $\text{K}_2\text{PtCl}_4$  (83.1 mg, 200  $\mu\text{mol}$ ; 1.2  $\text{cm}^3$ ) was added to a hot ethanolic solution (5  $\text{cm}^3$ ) of Hdpf (166.0 mg, 401  $\mu\text{mol}$ ); an orange precipitate formed immediately. The mixture was briefly boiled and allowed to stand at room temperature for 24 h, the precipitate was filtered off, washed with  $\text{EtOH}$  (2  $\times$  2  $\text{cm}^3$ ),  $\text{Et}_2\text{O}$  (3  $\times$  2  $\text{cm}^3$ ), petroleum ether (3  $\times$  2  $\text{cm}^3$ ) and air-dried, yielding 141.0 mg (64%) of an orange microcrystalline solid. IR,  $\tilde{\nu}/\text{cm}^{-1}$ : 1676 s, 1291 s, 1195 s, 1164 s, 1096 m, 999 s, 744 s, 709 s, 520 s (composite).

With stoichiometric amount of  $[\text{Pt}(\text{PhCN})_2\text{Cl}_2]$  used as the source of Pt(II), *trans*-**3** is also formed, but the product is contaminated with Hdpf (cf. *trans*-**1**; confirmed by elemental analysis and  $^{31}\text{P}$  NMR).

### 3.4. *Cis*- $[\text{Pt}(\text{Hdpf-P})_2\text{Cl}_2]$ , *cis*-3

The addition of a hot dichloromethane solution (5  $\text{cm}^3$ ) of Hdpf (166.0 mg, 401  $\mu\text{mol}$ ) to a solution of  $[\text{PtCl}_2(\text{cod})]$  (74.9 mg, 200  $\mu\text{mol}$ ) in hot dichloromethane (10  $\text{cm}^3$ ) provided a clear orange solution, which deposited an orange precipitate on standing

in refrigerator for 24 h. The precipitate was filtered off, washed with  $\text{EtOH}$  (2  $\times$  2  $\text{cm}^3$ ),  $\text{Et}_2\text{O}$  (3  $\times$  2  $\text{cm}^3$ ), petroleum ether (3  $\times$  2  $\text{cm}^3$ ) and dried on air yielding 204.8 mg (93%) of an orange microcrystalline solid. IR,  $\tilde{\nu}/\text{cm}^{-1}$ : 1674 s (composite), 1293 s, 1164 s, 1096 s, 999 s, 741 s, 690 s (composite), 480–510 s (composite).

## 4. Crystal structure determination

Single crystals of the *trans*-chloro complexes described above were grown by slow cooling of a hot solution in acetic acid (to give *trans*-**1** · 2 AcOH and *trans*-**3** · 2 AcOH) or in propionic acid (*trans*-**3**). Their identity was confirmed by IR spectra. The crystals were mounted on a glass fiber by epoxy cement. Single crystals of *cis*-**3** · 2  $\text{CH}_2\text{Cl}_2$  were obtained as follows. A hot solution of Hdpf (8.2 mg, 20  $\mu\text{mol}$ ) in dichloromethane (3  $\text{cm}^3$ ) was added to the solution of  $[\text{PtCl}_2(\text{cod})]$  (3.7 mg, 9.9  $\mu\text{mol}$ ) in the same solvent (3  $\text{cm}^3$ ) and the clear solution was brought to boiling. On standing at room temperature for several days, the mixture deposited well-developed microcrystals that disintegrated very rapidly on air. They were mounted into Lindenmann glass capillaries filled with  $\text{CH}_2\text{Cl}_2$  (under dichloromethane) fixed in position by a glass fiber dipped in epoxy cement and sealed. Despite these precautions, partial decomposition of all dried crystals was observed during the data collection. The results are therefore of low precision but the chemical picture is unambiguous.

All measurements were carried out on a CAD4-MACHIII four circle diffractometer at 296(1) K using graphite-monochromated  $\text{MoK}_\alpha$  radiation ( $\lambda = 0.71073$  Å) and  $\theta$ - $2\theta$  scan. Cell parameters were determined and refined by least-squares from 25 centered diffractions (for further details, see Table 3). The data for *trans*-**3** were numerically corrected for absorption after indexation of the crystal faces (AGNOSTIC [4]). In the case of *trans*-**3** · 2 AcOH and *cis*-**3** · 2  $\text{CH}_2\text{Cl}_2$ , the irregular shape of the crystal and/or measuring in the capillary did not allow this correction to be done. The absorption of *trans*-**1** · 2 AcOH was neglected.

All structures were solved by the heavy atom method (SHELXS86 [5]) followed by Fourier syntheses yielding the positions of all non-hydrogen atoms, and refined by full matrix least squares on  $F^2$  (SHELXL93 [6]). Aromatic hydrogens were fixed in theoretical positions and assigned  $U_{\text{iso}}(\text{H}) = 1.2 U_{\text{eq}}(\text{C})$  of the parent carbon. The carboxylic and methyl hydrogens of *trans*-complexes were located in difference maps and isotropically refined. With respect to disordered solvate molecules in *cis*-**3** · 2  $\text{CH}_2\text{Cl}_2$  from which only two could be located and refined, the formula should be better formulated as *cis*-**3** · (2 +  $x$ )  $\text{CH}_2\text{Cl}_2$ ,  $x \geq 0$ . Due to low-quality data in this case (fast scanning, decomposition, neglect of

Table 3

Crystallographic data for *trans-1* · 2 AcOH, *trans-3* · 2 AcOH, *trans-3* and *cis-3* · 2 CH<sub>2</sub>Cl<sub>2</sub>

Compound	<i>Trans-1</i> · 2 AcOH	<i>Trans-3</i> · 2 AcOH	<i>Trans-3</i>	<i>cis-3</i> · 2 CH <sub>2</sub> Cl <sub>2</sub>
Formula unit	C <sub>25</sub> H <sub>23</sub> O <sub>4</sub> PClFePd <sub>0.5</sub>	C <sub>25</sub> H <sub>23</sub> O <sub>4</sub> PClFePt <sub>0.5</sub>	C <sub>46</sub> H <sub>38</sub> O <sub>4</sub> P <sub>2</sub> Cl <sub>2</sub> Fe <sub>2</sub> Pt	C <sub>46</sub> H <sub>38</sub> O <sub>4</sub> P <sub>2</sub> Cl <sub>2</sub> Fe <sub>2</sub> Pt · 2 CH <sub>2</sub> Cl <sub>2</sub>
<i>M</i> (g mol <sup>-1</sup> )	562.9	607.3	1094.4	1264.3
Crystal system	Monoclinic	Monoclinic	Triclinic	Monoclinic
Space group	<i>P</i> 2 <sub>1</sub> / <i>n</i> (No. 14)	<i>P</i> 2 <sub>1</sub> / <i>n</i> (No. 14)	<i>P</i> <sub>1</sub> (No. 2)	<i>P</i> 2 <sub>1</sub> / <i>c</i> (No. 14)
<i>a</i> (Å); α (°)	10.7856(8)	10.884(1)	11.041(2); 101.40(1)	13.9941(9)
<i>b</i> (Å); β (°)	13.280(1); 96.925(7)	13.307(1); 96.879(7)	17.126(3); 105.64(1)	16.7920(9); 118.928(5)
<i>c</i> (Å); γ (°)	16.601(2)	16.533(1)	18.961(3); 103.11(1)	25.176(1)
<i>V</i> (Å <sup>3</sup> ); <i>Z</i>	2360.5(3); 4	2377.3(3); 4	3232.1(9); 3	5178.0(6); 4
θ range for cell parameters determination (%)	13–14	13–14	12.5–13	14–15
<i>D</i> <sub>c</sub> (g cm <sup>-3</sup> )	1.584	1.697	1.687	1.614
<i>F</i> (000)	1144	1208	1620	2472
Crystal size (mm <sup>3</sup> )	0.15 × 0.20 × 0.20	0.07 × 0.14 × 0.46	0.15 × 0.20 × 0.33	0.30 × 0.40 × 0.70
Crystal description	Orange prism	Irregular, orange	Orange prism	Orange bar
μ (mm <sup>-1</sup> ); <i>T</i> <sub>min</sub> , <i>T</i> <sub>max</sub>	1.22; –	3.77; –	4.14; 0.438, 0.609	3.66; –
2θ limit (°)	4–50	2–50	2–50	2–50
<i>h</i> , <i>k</i> , <i>l</i>	+ <i>h</i> , + <i>k</i> , ± <i>l</i>	+ <i>h</i> , + <i>k</i> , ± <i>l</i>	± <i>h</i> , + <i>k</i> , ± <i>l</i>	+ <i>h</i> , + <i>k</i> , ± <i>l</i>
Diffractions collected; <i>R</i> (σ) <sup>b</sup>	3924; 11.6	4283; 4.3	11368; 3.3	9080; 8.7
Diffractions unique; <i>R</i> <sub>int</sub> <sup>b</sup>	3716; 4.3	4056; 2.2	11360; 1.8	9077; 19.5
Diffractions observed	2138	2990	9030	5539
[ <i>F</i> <sub>o</sub> ≥ 4σ( <i>F</i> <sub>o</sub> )]				
Standard diffractions			3 monitored every 1 h	
Variation in standards (%)	2	3	4	9
Weighting scheme: <i>w</i> <sub>1</sub> , <i>w</i> <sub>2</sub> <sup>c</sup>	0.0141, 0.0	0.0485, 1.9040	0.0375, 2.9513	0.0211, 2.0400
Number of parameters	315	315	784	538
<i>R</i> <sub>all</sub> ( <i>F</i> ), <i>R</i> <sub>obs</sub> ( <i>F</i> ) <sup>b</sup> (%)	12.9, 4.3	6.4, 3.2	5.01, 2.81	16.2, 9.5
<i>wR</i> <sub>all</sub> ( <i>F</i> <sup>2</sup> ), <i>wR</i> <sub>all</sub> ( <i>F</i> <sup>2</sup> ) <sup>b</sup> (%)	7.3, 5.9	8.9, 8.0	7.20, 6.54	30.1, 24.8
GOF <sub>all</sub> <sup>b</sup>	1.02	1.07	1.02	1.04
(Δ/σ) <sub>max</sub>	0.000	0.000	0.002	0.000
Δρ (e Å <sup>-3</sup> )	0.43, –0.46	1.84, –1.37	1.59, –1.25	3.79, –3.87

<sup>a</sup>Data collected for *trans-3* were analytically corrected for absorption after indexation of the crystal faces (see Section 5; *T*<sub>min</sub>, *T*<sub>max</sub> values are given in this table).

<sup>b</sup> $R(F) = \sum(|F_o| - |F_c|) / \sum|F_o|$ ,  $wR(F^2) = \sum[(w(F_o^2 - F_c^2)^2) / (w(F_o^2)^2)]^{1/2}$ ,  $GOF = [\sum(w(F_o^2 - F_c^2)^2) / (N_{\text{diffs}} - N_{\text{params}})]^{1/2}$ ,  $R_{\text{int}} = \sum(F_o^2 - \langle F_o^2 \rangle) / \sum F_o^2$ ,  $R(\sigma) = \sum \sigma(F_o^2) / \sum F_o^2$ .

<sup>c</sup>Weighting scheme:  $w = [\sigma^2(F_o^2) + w_1 P^2 + w_2 P]^{-1}$ ;  $P = [\max(F_o^2) + 2 F_c^2] / 3$ .

absorption [see *R*<sub>int</sub>, *R*(σ) and the residuals in Table 3)], the aromatic hydrogens were fixed as above while carboxylic and solvate H-atoms could not be located at all. The relevant crystallographic data are given in Table 3. Full tables of atomic coordinates, thermal parameters and bond lengths and angles have been deposited at the Cambridge Crystallographic Data Centre.

## 5. Results and discussion

### 5.1. Syntheses and NMR spectra

The complexes, *trans*-dichloro-bis[(1'-diphenylphosphino)ferrocenecarboxylic acid-*P*]palladium(II), *trans-1*, *trans*-dibromo-bis[(1'-diphenylphosphino)ferrocenecarboxylic acid-*P*]palladium(II), *trans-2*, and *trans*-dichloro-bis[(1'-diphenylphosphino)ferrocenecarboxylic acid-*P*]platinum(II), *trans-3*, were prepared by the reac-

tion of stoichiometric amounts of ligand and the appropriate Pd(II) or Pt(II) compound. In toluene solution, M(C<sub>6</sub>H<sub>5</sub>CN)<sub>2</sub>Cl<sub>2</sub> (M=Pd(II) or Pt(II)) immediately after mixing with Hdpf deposits a fine precipitate of *trans-1*, *trans-3*, respectively, contaminated with free (non-coordinated) ligand. The reactions of K<sub>2</sub>MCl<sub>4</sub> (M=Pd(II) or Pt(II)) in aqueous ethanol yielded the same products as pure microcrystalline solids. Crystallization of the complexes from hot glacial acetic acid gives the solvates *trans-1* · 2 AcOH and *trans-3* · 2 AcOH in the quality suitable for X-ray analysis. In contrast, crystallization of *trans-3* from hot propionic acid yields single crystals of the non-solvated complex. Attempting to obtain the related *cis*-complexes, two equivalent Hdpf with η<sup>4</sup>-cycloocta-1,5-diene complexes of divalent palladium and platinum in dichloromethane were found to produce again *trans-2* in the case of Pd(II) but, for Pt(II) derivative, the expected complex *cis*-dichloro-bis[(1'-diphenylphosphino)ferrocenecarboxylic acid-*P*]platinum(II), *cis-3*, was isolated. The con-

certed substitution and isomerisation of the starting Pd(II) complex is the result of the well-known kinetic lability of square-planar Pd(II) phosphine complexes [7]. In contrast, *cis-3* is not isomerized but rather decomposed on prolonged boiling in acetic acid. The *cis*-complex was isolated as the dichloromethane solvate, *cis-3* · (2 + *x*) CH<sub>2</sub>Cl<sub>2</sub>. The solvent is readily lost on air; washing and air-drying at room temperature resulted in a non-stoichiometric composition with higher content of chlorine in comparison with the non-solvated derivative (%C 49.05, %H 3.47, %Cl 7.73; cf. Table 1). Analytically pure non-solvated *cis-3* was obtained by drying at 120°C for 5 h (elemental analysis is given in Table 1). The complexes are insoluble in all common solvents except dimethyl sulphoxide and hot carboxylic acids. They are air-stable in solid state, but slowly decompose in the DMSO or acidic solutions.

The <sup>1</sup>H, <sup>1</sup>H, <sup>1</sup>H-correlated and <sup>31</sup>P NMR spectra confirm that the solid-state molecular structures are maintained in *d*<sub>6</sub>-DMSO solution. As expected, the proton NMR spectra of the *trans*-complexes are very similar. Compared to the free ligand (for data obtained in C[<sup>2</sup>H]Cl<sub>3</sub> see Ref. [1]), the cyclopentadienyl (Cp) proton signals are slightly downfield-shifted and broadened with concomitant loss of the fine structure. This effect is more pronounced for the Ph<sub>2</sub>P-substituted cyclopentadienyl, the proton signals of which are mutually very close or even overlapped. On the other hand, the proton signals of both cyclopentadienyls in the *cis-3* complex are well separated, and its phenyl hydrogens display the expected 3:2 multiplet. The *trans-1* complex was further studied by <sup>13</sup>C APT and <sup>13</sup>C-HMQC NMR spectroscopy [<sup>13</sup>C APT signal (<sup>1</sup>H correlation in the case of CH protons)]; quaternary C: *C*<sub>*ipso*</sub>(CpPh<sub>2</sub>P) 72.1 t, <sup>1</sup>*J*(PC) = 27 Hz; *C*<sub>*ipso*</sub>(CpCOOH) 73.4 s; *C*<sub>*ipso*</sub>(Ph) 130.4 t, <sup>1</sup>*J*(PC) = 25 Hz; CO<sub>2</sub>H 171.3 s; CH: CpPPh<sub>2</sub> 73.8 s (4.54); 75.6 t, *J*(PC) = 5 Hz (4.52); CpCOOH 71.4 s (4.89); 73.8 s (4.76); Ph<sub>2</sub>P 128.0 t, *J*(PC) = 5 Hz; 130.6 s; 133.5 t, *J*(PC) = 6 Hz (all correlated with <sup>1</sup>H multiplet at 7.44–7.67). The <sup>13</sup>C signals of Cp-PPh<sub>2</sub> carbons appear as triplets indicating that <sup>*n*</sup>*J*(PC) ≈ <sup>*n*+2</sup>*J*(PC) [the AXX' spin system; A = <sup>13</sup>C, X = <sup>31</sup>P]. This is most likely the result of a conjugation within the Cp-P(Ph)<sub>2</sub>-M-P(Ph)<sub>2</sub>-Cp moiety (see below). The <sup>31</sup>P{<sup>1</sup>H} spectra of the complexes consist of one singlet with typical <sup>195</sup>Pt-satellites for Pt-complexes. The position of the singlet is markedly downfield-shifted relatively to the free ligand, for *trans*-complexes even more than for the *cis*-derivative: Δ = δ<sub>complex</sub> - δ<sub>free ligand</sub>; Δ<sub>p</sub>, ppm: *trans-1*, 35.1; *trans-2*, 34.0; *trans-3*, 30.9; *cis-3*, 27.6 (δ<sub>p</sub>(Hdpf) -18.4 at the conditions given in Table 1). These values alone cannot be taken as a safe indication of the coordination geometry due to their sensitivity to changes in hybridization, electron density, conjugation, etc. [8]. However, the coupling constants <sup>1</sup>*J*(<sup>195</sup>Pt, <sup>31</sup>P) unambiguously show that the solid-state

arrangement is retained in solution since <sup>1</sup>*J*(Pt, P; *cis*) is always greater than <sup>1</sup>*J*(Pt, P; *trans*) for complexes of the [M(PR<sub>3</sub>)<sub>2</sub>Y<sub>2</sub>] type where Y is a substituent of low trans-influence such as halide [9]. As an illustration, the data for *cis-3* are in perfect agreement with the complex of the related *cis*-chelating ligand, [PtCl<sub>2</sub>(1,1'-bis(diphenylphosphino)ferrocene-*P*, *P'*)]: <sup>1</sup>*J*(<sup>195</sup>Pt, <sup>31</sup>P) = 3769 Hz, Δ<sub>p</sub> = 29.9 [10].

## 5.2. FAB-MS spectra

In FAB mass spectra of all complexes, peaks due to [M-CpCO<sub>2</sub>-*n*X]<sup>+</sup> (*n* = 0, 1, 2) and [Hdpf]<sup>+</sup> were observed. For *cis-3*, the positive fragment ions [M - *n*X]<sup>+</sup> (*n* = 1, 2), formed by sequential loss of halogen, were much more intense than those for the *trans*-complexes. The intensity of the molecular ion of *cis-3* is significantly lower than that of all *trans*-complexes. Apparently, this is the consequence of the stronger *trans*-effect of phosphines compared to halides, supported by the mutual sterical destabilization of the *cis*-phosphines. In the *trans*-complexes, peaks of the [HdpfMX]<sup>+</sup> (M = Pd, Pt) and [M-CpCO<sub>2</sub>Fe-CpCO<sub>2</sub>-*n*X]<sup>+</sup> (*n* = 0, 1, 2) fragments corresponding to further decomposition were identified. The preferred loss of the halide ligands and the carboxylated Cp-rings (alone or together with the iron atom) can be taken as a further support for conjugation within the highly stable Cp-P(Ph)<sub>2</sub>-M-P(Ph)<sub>2</sub>-Cp moiety through M ← P π-back donation and simultaneous strong σ-bonding, as proposed from the NMR spectra.

## 5.3. Crystal structures of *trans-1*, *trans-1* · 2 AcOH, *trans-3* · 2 AcOH and *cis-3* · 2 CH<sub>2</sub>Cl<sub>2</sub>

The results of crystal structure determination of four complexes are summarized in Figs. 1–4 and Tables 4–7. At first sight, the structures are unexceptional and of the ordinary square-planar MX<sub>2</sub>(PR<sub>3</sub>)<sub>2</sub> type (M = Pd, Pt; X = halide). The ferrocenyl ligand behaves as a monodentate phosphine in all cases, and its carboxyl group participates in hydrogen bonding whose organization, however, varies substantially from compound to compound. The structure of the coordinated ligand is similar to that of the free one [1], being characterized by nearly parallel cyclopentadienyl rings. The principal difference between the free and complexed ligand is in the mutual conformation of the substituents at the cyclopentadienyls which is, in contrast to the free ligand [1], nearly staggered in all complexes. As expected, the arrangement of the substituents at phosphorus is also changed remarkably on coordination.

The complexes *trans-1* · 2 AcOH and *trans-3* · 2 AcOH are isostructural. Their coordination polyhedron is exactly (by symmetry) planar with bond angles differing only little from 90°. On going from Pd to Pt, there is

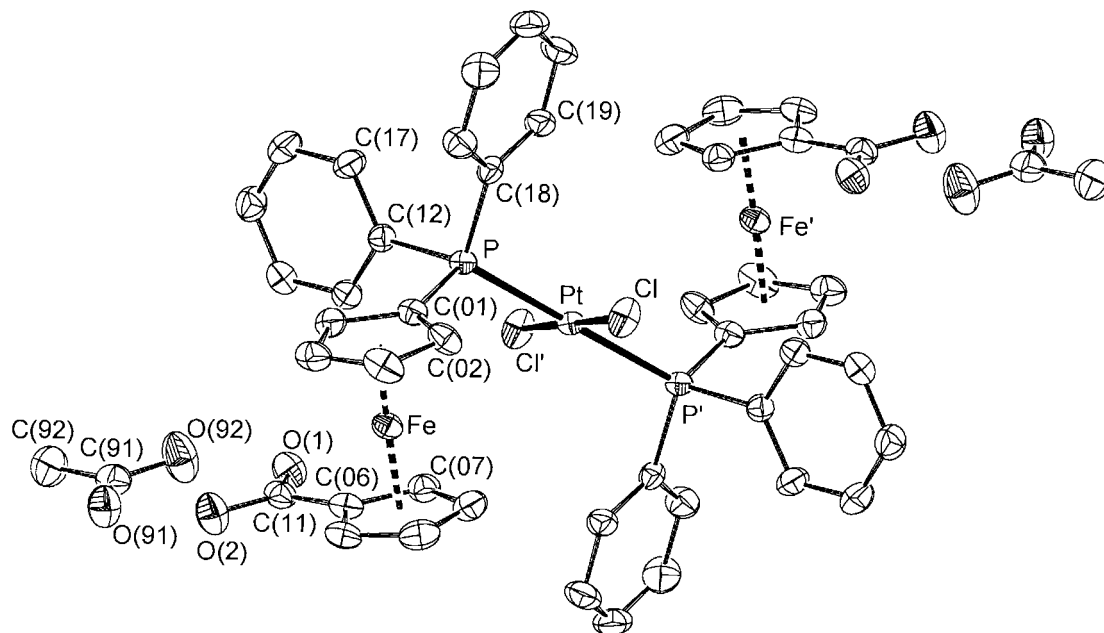


Fig. 1. Perspective view of *trans*-3 · 2 AcOH with atom labelling (PLATON-plot, 30% probability).

a small but significant shortening of the M–P and lengthening of the M–Cl distance, in accordance with a softer character of Pt(II) compared to Pd(II). As indicated by the torsion angle  $\tau$  (defined by carboxylic carbon, centroids of the cyclopentadienyls and phospho-

rus) which is  $81.8(3)^\circ$  for Pd and  $82.1(3)^\circ$  for Pt complex, the conformation of the substituents is synclinal when looking perpendicularly to the cyclopentadienyl planes. The carboxyl group participates in the usual double hydrogen bonding to the approximately planar

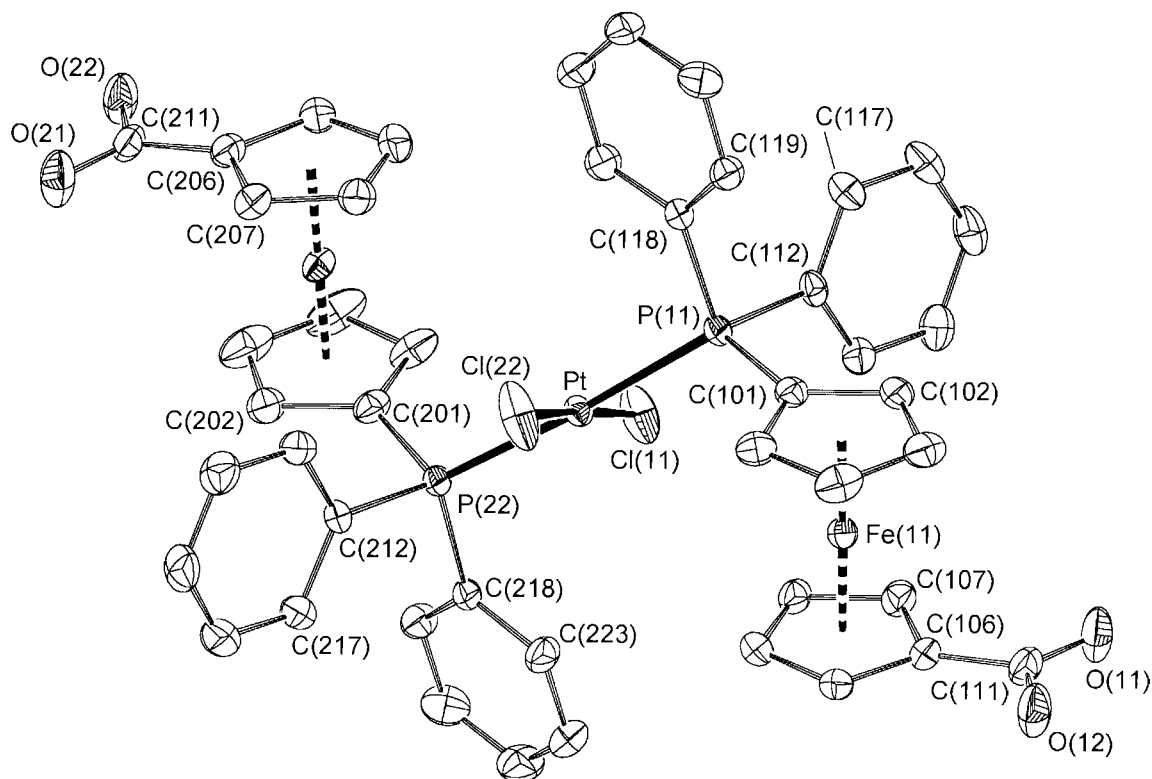


Fig. 2. Perspective view of *trans*-3 (molecule B) with atom labelling (PLATON-plot, 30% probability).

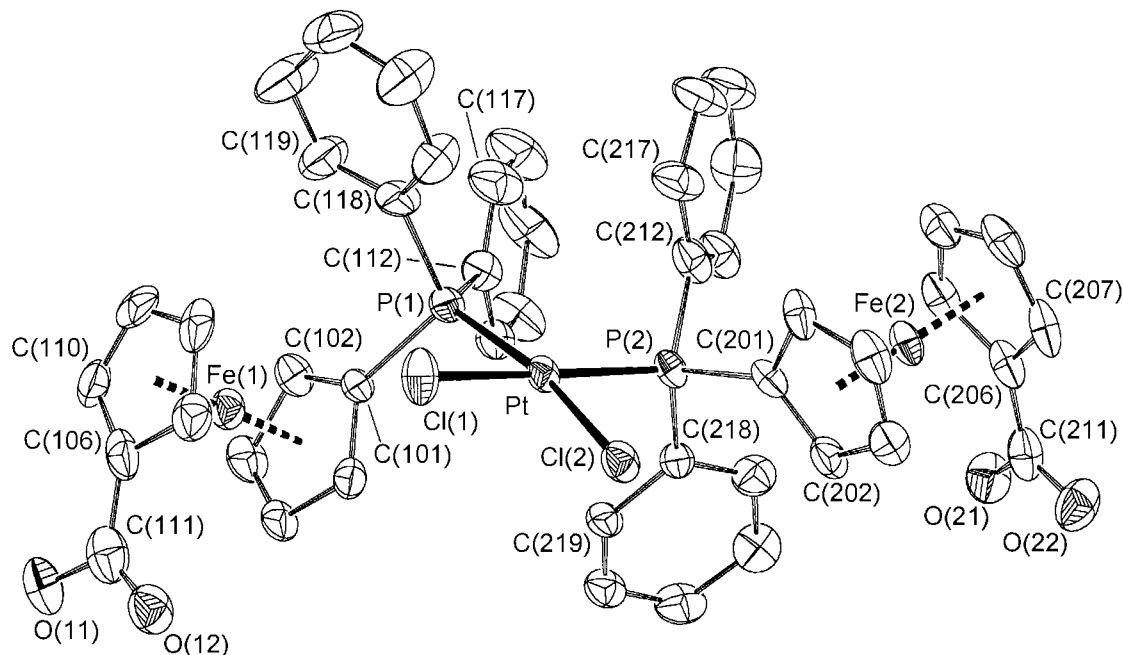


Fig. 3. Perspective view of *cis*-**3** · 2 CH<sub>2</sub>Cl<sub>2</sub> with atom labelling (PLATON-plot, 30% probability). Solvate dichloromethane was omitted.

molecule of acetic acid with the following parameters of the hydrogen bonds. For *trans*-**1** · 2 AcOH [for *trans*-**3** · 2 AcOH in square brackets]: O(1) ··· O(92) 2.622(7) [2.615(7)] Å, O(92)–H(91) 0.75(6) [0.78(7)] Å, O(1) ··· H(91) 1.89(6) [1.84(7)] Å, O(92)–H(91) ··· O(1) 168(8) [172(8)]°; O(2) ··· O(91) 2.651(7) [2.663(8)] Å, O(2)–H(90) 0.74(7) [0.88(8)] Å, O(91) ··· H(90) 1.91(7) [1.79(8)] Å, O(2)–

H(90) ··· O(91) 172(8) [168(9)]°. The packing of the solvates is thus molecular with no other contacts except those at the van der Waals level.

Interestingly, the crystallization of *trans*-**3** from propionic acid (and also from formic acid, with partial reduction to Pt metal) produces unsolvated *trans*-**3**. No reason for this anomaly could be seen by inspection of the environment of the methyl group of the acetic acid, as enough place is available here for the further carbon atom. The asymmetric part of the unit cell is composed of one-half of molecule (**A**) with its Pt atom in special

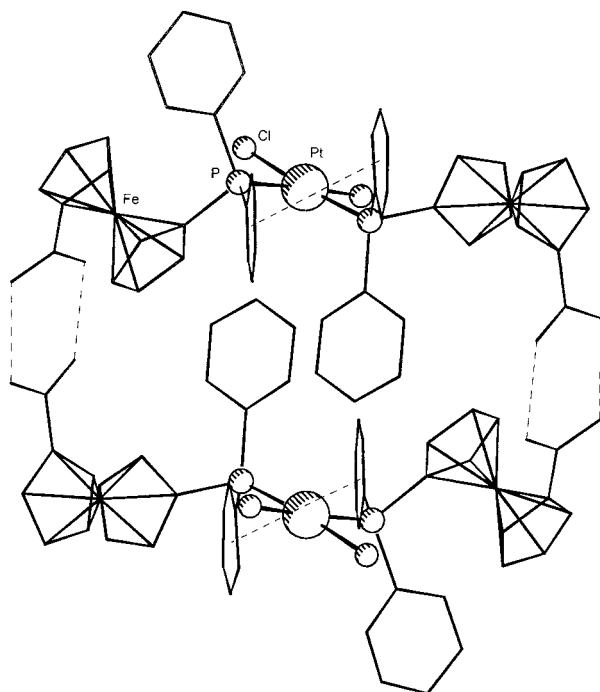


Fig. 4. Perspective view of the dimer of *cis*-**3** · 2 CH<sub>2</sub>Cl<sub>2</sub> (arbitrary atom diameters); hydrogen bonding and  $\pi$ – $\pi$  interaction drawn as dotted lines. Solvate not displayed.

Table 4  
Selected bond lengths (Å) and angles (°) for *trans*-**1** · 2 AcOH

Pd–Cl	2.296(1)	Cl–Pd–P	86.24(5)
Pd–P	2.363(1)	Pd–P–C(01)	118.8(2)
P–C(01)	1.811(5)	Pd–P–C(12)	119.1(2)
P–C(12)	1.815(5)	Pd–P–C(18)	108.9(2)
P–C(18)	1.813(5)	C(01)–P–C(12)	100.9(2)
		C(01)–P–C(18)	104.0(2)
		C(12)–P–C(18)	103.2(2)
mean Fe–C(Cp)	2.036(7)	mean C–C–C(Cp)	108.0(7)
mean C–C(Cp)	1.41(1)	mean C–C–C(Ph)	120(1)
mean C–C(Ph)	1.37(1)		
C(06)–C(11)	1.465(8)	O(1)–C(11)–O(2)	124.2(6)
C(11)–O(1)	1.222(6)	O(1)–C(11)–C(06)	121.7(6)
C(11)–O(2)	1.309(7)	O(2)–C(11)–C(06)	114.1(6)
O(2)–H(90)	0.74(6)	C(11)–O(2)–H(90)	106(6)
C(91)–O(91)	1.221(7)	O(91)–C(91)–O(92)	121.4(7)
C(91)–O(92)	1.305(8)	C(91)–O(92)–H(91)	109(6)
O(92)–H(91)	0.75(6)	H(92)–C(92)–H(93)	109(7)
C(91)–C(92)	1.49(1)	H(92)–C(92)–H(94)	119(9)
C(92)–H(92)	0.86(8)	H(93)–C(92)–H(94)	114(8)
C(92)–H(93)	0.89(6)		
C(92)–H(94)	0.85(8)		

Table 5  
Selected bond lengths (Å) and angles (°) for *trans*-**3**·2 AcOH

Pt–Cl	2.308(2)	Cl–Pt–P	86.11(5)
Pt–P	2.340(1)	Pt–P–C(01)	118.1(2)
P–C(01)	1.818(5)	Pt–P–C(12)	118.7(2)
P–C(12)	1.826(6)	Pt–P–C(18)	110.3(2)
P–C(18)	1.823(6)	C(01)–P–C(12)	100.3(3)
		C(01)–P–C(18)	103.7(3)
		C(12)–P–C(18)	103.7(3)
mean Fe–C(Cp)	2.044(9)	mean C–C–C(Cp)	108.0(8)
mean C–C(Cp)	1.42(1)	mean C–C–C(Ph)	120(1)
mean C–C(Ph)	1.38(1)		
C(06)–C(11)	1.464(9)	O(1)–C(11)–O(2)	122.8(6)
C(11)–O(1)	1.238(7)	O(1)–C(11)–C(06)	121.4(6)
C(11)–O(2)	1.311(7)	O(2)–C(11)–C(06)	115.7(6)
O(2)–H(90)	0.88(8)	C(11)–O(2)–H(90)	109(5)
C(91)–O(91)	1.204(9)	O(91)–C(91)–O(92)	123.1(7)
C(91)–O(92)	1.29(1)	C(91)–O(92)–H(91)	108(6)
O(92)–H(91)	0.78(7)	H(92)–C(92)–H(93)	123(7)
C(91)–C(92)	1.50(1)	H(92)–C(92)–H(94)	94(7)
C(92)–H(92)	1.1(1)	H(93)–C(92)–H(94)	106(8)
C(92)–H(93)	1.0(1)		
C(92)–H(94)	0.89(8)		

position, and of molecule (**B**), located in a general position. The structure of the two molecules is similar, differing mostly by 0.025(2) Å in bond lengths, by 1.3(5)° in bond angles and by 5.4(2)° in the dihedral angle of the vicinal phenyl groups; further, the coordination polyhedron of molecule **B** is slightly non-planar: the largest perpendicular distance of the polyhedron atoms from their least-squares plane is 0.075(6) Å for

P(22). In comparison to the structure of the solvate, the coordination polyhedrons of the unsolvated complex vary only slightly while the conformation of the ferrocene moiety and especially the crystal packing is markedly different. The ferrocene substituents become anticlinal [ $\tau = 149.1(2)^\circ$  for **A**,  $141.1(2)^\circ$  and  $144.8(2)^\circ$  for **B**] and, obviously because of the absence of solvent, the molecules are linked into infinite zigzag chains through double hydrogen bonds between the opposite carboxyl groups. The parameters of the hydrogen bonds are: for molecule **A**, O(2)  $\cdots$  O(1<sup>I</sup>) 2.634(6) Å, O(2)–H(90) 0.59(6) Å, O(1<sup>I</sup>)  $\cdots$  H(90) 2.05(6) Å, O(2)–H(90)  $\cdots$  O(1<sup>I</sup>) 174(9)°, I:  $1 - x, 1 - y, -z$ ; for molecule **B**, O(12)  $\cdots$  O(21<sup>II</sup>) 2.625(5) Å, O(12)–H(91) 0.74(8) Å, O(21<sup>II</sup>)  $\cdots$  H(91) 1.90(8) Å, O(12)–H(91)  $\cdots$  O(21<sup>II</sup>) 170(9)°, O(22<sup>II</sup>)  $\cdots$  O(11) 2.600(6) Å, O(22)–H(92) 0.72(9) Å, O(11)  $\cdots$  H(92<sup>II</sup>) 1.89(9) Å, O(22<sup>II</sup>)–H(92<sup>II</sup>)  $\cdots$  O(11) 170(10)°, II:  $1 + x, 1 + y, z$ .

The hydrogen-bonded chains run parallel to the crystallographic *ab*-plane and are stacked in a staggered manner such that the molecules **A** lie approximately within this plane and two symmetry-related molecules **B** in approximately one and two thirds of the *c*-axis; hence, the value of  $Z = 3$  which is uncommon for the  $P\bar{1}$  space group but not unprecedented even among Pt(II) complexes [11,12]. Again, there are no further notable interactions between the layers; the conformation of the phenyl groups, however, is forced such as to avoid unfavourable intermolecular contacts.

Table 6  
Selected bond lengths (Å) and angles (°) for *trans*-**3**

Pt(1)–Cl(1)	2.299(1)	Pt(2)–Cl(11)	2.295(1)	Pt(2)–Cl(22)	2.270(1)
Pt(1)–P(1)	2.328(1)	Pt(2)–P(11)	2.319(1)	Pt(2)–P(22)	2.327(1)
P(1)–C(01)	1.809(5)	P(11)–C(101)	1.804(5)	P(22)–C(201)	1.805(4)
P(1)–C(12)	1.825(5)	P(11)–C(112)	1.820(4)	P(22)–C(212)	1.830(4)
P(1)–C(18)	1.814(4)	P(11)–C(118)	1.819(4)	P(22)–C(218)	1.813(4)
Mean Fe–C(Cp)	2.03(1)		2.04(1)		2.035(6)
Mean C–C(Cp)	1.41(1)		1.42(1)		1.41(1)
Mean C–C(Ph)	1.37(1)		1.38(1)		1.378(7)
C(06)–C(11)	1.464(7)	C(106)–C(111)	1.458(7)	C(206)–C(211)	1.460(6)
C(11)–O(1)	1.232(7)	O(11)–C(111)	1.238(6)	C(211)–O(21)	1.239(6)
C(11)–O(2)	1.297(7)	O(12)–C(111)	1.276(6)	C(211)–O(22)	1.280(6)
Cl(1)–Pt(1)–P(1)	85.71(5)	Cl(11)–Pt(2)–P(11)	93.22(5)	Cl(22)–Pt(2)–P(11)	86.32(4)
		Cl(11)–Pt(2)–P(22)	88.75(5)	Cl(22)–Pt(2)–P(22)	91.92(4)
		Cl(11)–Pt(2)–Cl(22)	176.96(7)	P(11)–Pt(2)–P(22)	175.71(4)
Pt(1)–P(1)–C(01)	118.4(2)	Pt(2)–P(11)–C(101)	115.7(2)	Pt(2)–P(22)–C(201)	117.9(1)
Pt(1)–P(1)–C(12)	119.2(2)	Pt(2)–P(11)–C(112)	118.6(2)	Pt(2)–P(22)–C(212)	120.1(1)
Pt(1)–P(1)–C(18)	108.0(2)	Pt(2)–P(11)–C(118)	110.5(1)	Pt(2)–P(22)–C(218)	108.4(1)
C(01)–P(1)–C(12)	100.4(2)	C(101)–P(11)–C(112)	101.7(2)	C(201)–P(22)–C(212)	101.1(2)
C(01)–P(1)–C(18)	104.5(2)	C(101)–P(11)–C(118)	103.9(2)	C(201)–P(22)–C(218)	105.5(2)
C(12)–P(1)–C(18)	104.7(2)	C(112)–P(11)–C(118)	104.9(2)	C(212)–P(22)–C(218)	101.8(2)
Mean C–C–C(Cp)	108.0(5)		108.0(8)		108.0(6)
Mean C–C–C(Ph)	120.0(8)		120.0(7)		120.0(9)
O(1)–C(11)–O(2)	123.8(5)	O(11)–C(111)–O(12)	122.9(5)	O(21)–C(211)–O(22)	123.2(5)
O(1)–C(11)–C(06)	122.3(5)	O(11)–C(111)–C(106)	120.2(4)	O(21)–C(211)–C(206)	120.1(5)
O(2)–C(11)–C(06)	114.0(6)	O(12)–C(111)–C(106)	116.9(4)	O(22)–C(211)–C(206)	116.7(5)
C(11)–O(2)–H(90)	109(7)	C(111)–O(12)–H(91)	117(7)	C(211)–O(22)–H(92)	112(8)

Table 7  
Selected bond lengths (Å) and angles (°) for *cis-3*·2 CH<sub>2</sub>Cl<sub>2</sub>

Pt–P(1)	2.257(4)	P(2)–Pt–P(1)	98.7(2)
Pt–P(2)	2.256(4)	Cl(1)–Pt–Cl(2)	85.8(2)
Pt–Cl(1)	2.335(5)	P(1)–Pt–Cl(1)	85.9(2)
Pt–Cl(2)	2.345(4)	P(2)–Pt–Cl(1)	174.2(2)
		P(1)–Pt–Cl(2)	169.7(2)
		P(2)–Pt–Cl(2)	90.0(2)
P(1)–C(101)	1.82(1)	C(101)–P(1)–C(118)	110.8(8)
P(1)–C(118)	1.83(2)	C(101)–P(1)–C(112)	98.3(8)
P(1)–C(112)	1.87(2)	C(118)–P(1)–C(112)	102.1(9)
P(2)–C(201)	1.78(2)	C(101)–P(1)–Pt	108.4(5)
P(2)–C(218)	1.81(2)	C(118)–P(1)–Pt	113.7(6)
P(2)–C(212)	1.84(2)	C(112)–P(1)–Pt	122.4(6)
		C(201)–P(2)–C(218)	107.0(7)
O(11)–C(111)	1.34(2)	C(201)–P(2)–C(212)	101.6(7)
O(12)–C(111)	1.28(3)	C(218)–P(2)–C(212)	108.2(8)
C(106)–C(111)	1.48(3)	C(201)–P(2)–Pt	110.7(5)
O(21)–C(211)	1.26(2)	C(218)–P(2)–Pt	112.9(5)
O(22)–C(211)	1.26(2)	C(212)–P(2)–Pt	115.6(7)
C(206)–C(211)	1.44(3)		
		O(12)–C(111)–O(11)	122(2)
Cl(1A)–C(1)	1.72(4)	O(11)–C(111)–C(106)	117(2)
Cl(1B)–C(1)	1.70(4)	O(12)–C(111)–C(106)	121(2)
Cl(2A)–C(2)	1.59(4)	O(21)–C(211)–O(22)	124(2)
Cl(2B)–C(2)	1.79(4)	O(21)–C(211)–C(206)	120(2)
		O(22)–C(211)–C(206)	116(2)
		Cl(1B)–C(1)–Cl(1A)	107(2)
		Cl(2A)–C(2)–Cl(2B)	109(3)
Mean Fe–C(Cp)	2.04(2)	mean C–C–C(Cp)	108(2)
Mean C–C(Cp)	1.42(3)	mean C–C–C(Ph)	120(2)
Mean C–C(Ph)	1.39(3)		

The structure of *cis-3* also displays gross features of this type of complexes. Due to steric requirements of the bulky *cis*-phosphines, the coordination polyhedron is distorted both in bond angles and in overall non-planarity: the maximal perpendicular distance of the atoms constituting the coordination polyhedron from their least-squares plane is 0.139(5) Å for Cl(1). The conformation of the ferrocenyl substituents is again anticlinal with  $\tau$ -values of 146.3(6)° and 143.2(7)°. There are two remarkable interactions between the functional groups of the ligands. First, one phenyl group of the ligand exhibits a graphite-like intramolecular  $\pi$ -contact to its counterpart phenyl of the second phosphine. The contact has a bonding character [13] since the phenyl groups are nearly coplanar [at a dihedral angle of 3.9(5)°] and slipped, resulting in the mean distance of 3.64(2) Å for the corresponding carbons. This is a relatively common case among Pt(II) complexes with phenyl-substituted *cis*-phosphines [12].<sup>1</sup> The second interaction is spectacular, but quite normal when the whole molecule is looked upon as a little exotic  $\alpha$ ,  $\omega$ -dicarboxylic acid:

<sup>1</sup> Cambridge Structure Database CODENs for structures with closely similar geometry of the  $\pi$ - $\pi$  interaction: BAZKUI, BZP-NPU, EBZPPT10, MBZPBT10.

the molecules are paired into centrosymmetric dimers by two double hydrogen bonds between their peripheral carboxyl groups, resulting in a formal 28-membered macrocycle (Fig. 4). The parameters of the double hydrogen bridge are as follows: O(11)···O(22<sup>III</sup>) 2.64(2) Å, O(12)···O(21<sup>III</sup>) 2.64(2) Å, III:  $-x$ ,  $-y$ ,  $-z$ ; hydrogen atoms were not localized. Both these interactions are reflected on the conformation of the ligand which differs considerably from that in the *trans*-complexes: while the appropriate bond and torsion angles around phosphorus in the *trans*-series average within  $\pm 1.5^\circ$  and  $\pm 3^\circ$  respectively, the corresponding values for the *cis*-derivative differ from these averages by as much as 12° in bond angles and 19° in dihedral angles, the largest deviations appearing for the  $\pi$ -bonded phenyls. Finally, the dimeric units are packed mostly at the van der Waals distances but with channels large enough to incorporate loosely held solvent molecules.

## Acknowledgements

The support of this work by Grant Agency of Czech Republic (Grant No. 203/96/0111) and by Grant Agency of Charles University (Grant No. 209/1996) is gratefully acknowledged. The author (M.P.) thanks Dr. Vladimír Havlíček for providing access to mass spectrometer.

## References

- [1] J. Podlaha, P. Štěpnička, J. Ludvík, I. Císařová, *Organometallics* 15 (1996) 543.
- [2] J. Podlahová, B. Kratochvíl, J. Podlaha, J. Hašek, *J. Chem. Soc., Dalton. Trans.* (1985) 2393 and references therein.
- [3] D. Drew, J.R. Doyle, A.G. Shaver, in: F.A. Cotton (Ed.), *Inorganic Syntheses*, Vol. 13, McGraw-Hill, New York, 1972, p. 47.
- [4] D.H. Templeton, L.K. Templeton, AGNOSTIC, Program for Absorption Correction, Univ. of California, Berkeley, 1978.
- [5] G.M. Sheldrick, SHELX 86, Program for the Solution of Crystal Structures, Univ. of Göttingen, Göttingen, 1986.
- [6] G.M. Sheldrick, SHELXL 93, Program for Crystal Structure Refinement from Diffraction Data, Univ. of Göttingen, Göttingen, 1993.
- [7] F.R. Hartley, *The Chemistry of Platinum and Palladium*, Appl. Sci., London (1973), pp. 133, 313–315.
- [8] P.S. Pregosin, R.W. Kunz, in: P. Diehl, E. Fluck, R. Kosfeld (Eds.), *NMR—Basic Principles and Progress: <sup>31</sup>P and <sup>13</sup>C NMR of Transition Metal Phosphine Complexes*, Vol. 16, Springer, Berlin, 1979, pp. 47–56.
- [9] A. Zschunke, *Z. Chem.* 29 (1989) 34.
- [10] B. Corain, B. Longato, G. Favero, D. Ajò, G. Pilloni, U. Russo, F.R. Kreisl, *Inorg. Chim. Acta* 157 (1989) 259.
- [11] Cambridge Structure Database CODENs: GIMRID, IPAPTC, KAYKIE01, OXOXPT, VUBTAN, YUNTEG.
- [12] F.H. Allen, O. Kennard, *Chem. Design Automation News* 8 (1993) pp. 1, 31.
- [13] G.R. Desiraju, *Angew. Chem., Int. Ed. Engl.* 34 (1996) 2311.